



# Spin-Valley Relaxation and Exciton-Induced Depolarization Dynamics of Landau-Quantized Electrons in MoSe<sub>2</sub> Monolayer

## Journal Article

### Author(s):

Smolenski, Tomasz ; Watanabe, Kenji; Taniguchi, Takashi; Kroner, Martin ; Imamoglu, Atac

### Publication date:

2022-03-25

### Permanent link:

<https://doi.org/10.3929/ethz-b-000539251>

### Rights / license:

[Creative Commons Attribution 4.0 International](#)

### Originally published in:

Physical Review Letters 128(12), <https://doi.org/10.1103/physrevlett.128.127402>

### Funding acknowledgement:

204076 - Strongly correlated electrons in van der Waals heterostructures: an optical investigation (SNF)  
185902 - QSIT - Quantum Science and Technology (SNF)

## Spin-Valley Relaxation and Exciton-Induced Depolarization Dynamics of Landau-Quantized Electrons in MoSe<sub>2</sub> Monolayer

T. Smoleński<sup>1,\*</sup>, K. Watanabe,<sup>2</sup> T. Taniguchi,<sup>3</sup> M. Kroner,<sup>1</sup> and A. Imamoglu<sup>1</sup>

<sup>1</sup>*Institute for Quantum Electronics, ETH Zürich, CH-8093 Zürich, Switzerland*

<sup>2</sup>*Research Center for Functional Materials, National Institute for Materials Science, Tsukuba, Ibaraki 305-0044, Japan*

<sup>3</sup>*International Center for Materials Nanoarchitectonics, National Institute for Materials Science, Tsukuba, Ibaraki 305-0044, Japan*



(Received 7 July 2021; revised 5 December 2021; accepted 26 January 2022; published 24 March 2022)

Nonequilibrium dynamics of strongly correlated systems constitutes a fascinating problem of condensed matter physics with many open questions. Here, we investigate the relaxation dynamics of Landau-quantized electron system into spin-valley polarized ground state in a gate-tunable MoSe<sub>2</sub> monolayer subjected to a strong magnetic field. The system is driven out of equilibrium with optically injected excitons that depolarize the electron spins and the subsequent electron spin-valley relaxation is probed in time-resolved experiments. We demonstrate that both the relaxation and light-induced depolarization rates at millikelvin temperatures sensitively depend on the Landau level filling factor: the relaxation is enhanced whenever the electrons form an integer quantum Hall liquid and slows down appreciably at noninteger fillings, while the depolarization rate exhibits an opposite behavior. Our findings suggest that spin-valley dynamics may be used as a tool to investigate the interplay between the effects of disorder and strong interactions in the electronic ground state.

DOI: [10.1103/PhysRevLett.128.127402](https://doi.org/10.1103/PhysRevLett.128.127402)

Over the last decade, there has been an explosive growth of research investigating two-dimensional semiconductors such as transition metal dichalcogenide (TMD) monolayers and their van der Waals heterostructures [1,2]. This system features unique optical properties owing to ultralarge exciton binding energy [3,4] as well as the existence of valley pseudospin degree of freedom [5–8] that is locked to the spin by a strong spin-orbit coupling. In parallel, TMD heterostructures offer a fertile ground for investigations of correlated electronic states that arise due to strong Coulomb interactions. This has been recently demonstrated by several breakthrough experiments [9–13] showing evidence of the formation of Mott-like correlated insulating (CI) states in twisted TMD hetero- and homobilayers. Unlike magic-angle twisted bilayer graphene (MATBG) [14–16], even fractional fillings of the TMD moiré superlattices show a CI behavior, providing direct evidence for the dominant role played by long-range interactions that break discrete translation symmetry [10,17]. Remarkably, even in TMD monolayers the Coulomb interactions between the itinerant electrons at densities not exceeding a few  $10^{11} \text{ cm}^{-2}$  turn out to be strong enough to allow the electrons to spontaneously break continuous translational

symmetry and form a Wigner crystal (WC), as recently discovered by Refs. [18,19]. In parallel, the formation of fractional quantum Hall states in a TMD monolayer has also been evidenced under strong magnetic fields ( $B$ ) [20].

Despite a rapid progress in exploration of strong electronic correlations in MATBG and TMD heterostructures, the prior research focused primarily on the ground-state properties. Many of the interesting open questions in condensed matter physics, however, concern the non-equilibrium dynamics of strongly correlated systems. In the context of TMD systems, a key question that would determine the utility of the valley degree of freedom is the relaxation dynamics of an electron or hole system following an intervalley excitation. For WSe<sub>2</sub>/WS<sub>2</sub> heterobilayer, such a hole spin-valley relaxation was shown to slow down upon the formation of a CI state at an integer filling of the moiré superlattice [10]. In case of TMD monolayers, even though the spin-valley relaxation dynamics has been investigated in several prior experiments [21–28], the effects of ground-state electronic correlations on this relaxation remained elusive.

Here, we study the temporal dynamics of an excited state of Landau-quantized electron system in a charge-tunable MoSe<sub>2</sub> monolayer under high  $B = 14 \text{ T}$ . This state is prepared optically by means of a resonant injection of excitons that interact with itinerant electrons and lead to sizable depolarization of their spins. Our time-resolved pump-probe experiments reveal that both the light-induced depolarization dynamics as well as the rate of subsequent electronic spin relaxation exhibit striking,

---

*Published by the American Physical Society under the terms of the Creative Commons Attribution 4.0 International license. Further distribution of this work must maintain attribution to the author(s) and the published article's title, journal citation, and DOI.*

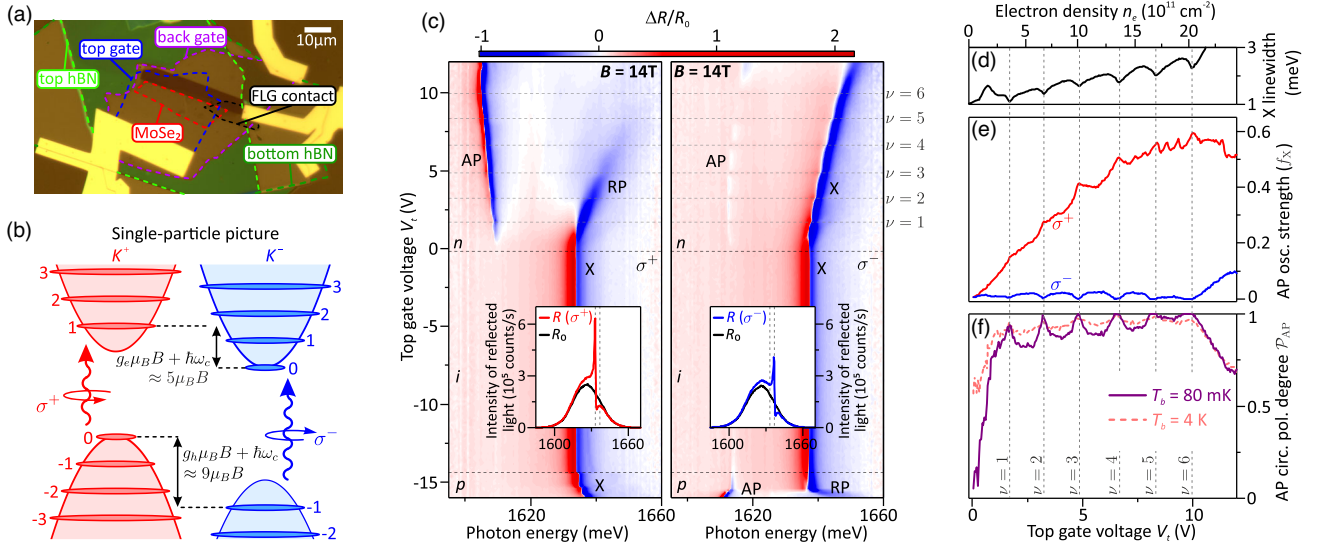


FIG. 1. (a) Optical micrograph of the investigated device. (b) Schematic illustrating the lowest-energy spin-orbit-split bands in a MoSe<sub>2</sub> monolayer at a finite  $B$  in a single-particle approximation. The energy splitting  $g_{e,h}^* \mu_B B$  between the lowest electron (hole) LLs in the  $K^+$  and  $K^-$  valleys is given by the sum of the cyclotron energy  $\hbar\omega_c = \hbar e B / m_{e,h}^*$  and the electron (hole) Zeeman term, corresponding to an effective  $g$  factor of  $g_e^* \approx 5$  ( $g_h^* \approx 9$ ) [2,41–43] for the electron and hole effective masses  $m_e^* \approx 0.7m_0$  [44] and  $m_h^* \approx 0.6m_0$  [45,46]. (c) Color-scale maps showing the  $V_t$  evolution of  $\Delta R/R_0 = (R - R_0)/R_0$  spectra measured at  $T_b = 80$  mK,  $B = 14$  T in  $\sigma^+$  (left) and  $\sigma^-$  (right) polarizations. Horizontal dashed lines mark the onsets of electron and hole doping as well as subsequent integer filling factors at  $V_t > 0$ . The insets depict example reflectance spectra  $R$  and  $R_0$  acquired, respectively, on and off the MoSe<sub>2</sub> flake at  $V_t = -1$  V, based on which  $\Delta R/R_0$  is evaluated (vertical dashed lines mark the energies of Zeeman-split excitons). (d)–(f) Electron-density dependence of the linewidth of  $\sigma^-$ -polarized exciton (d), oscillator strengths of AP<sub>±</sub> resonances (e), and the AP circular polarization degree (f) determined based on fitting the line shapes of the transitions in panel (c) (see SM [32]). The AP oscillator strengths are expressed relative to the exciton oscillator strength  $f_X$  at charge neutrality. The dashed line in (f) presents  $\mathcal{P}_{AP}$  determined at the same spot and  $B$ , but at elevated  $T_b = 4$  K.

periodic oscillations with the Landau level (LL) filling factor  $\nu$  at millikelvin temperatures. The fast relaxation for integer quantum Hall (IQH) states together with its striking slowing down for a WC at  $\nu \lesssim 0.5$  [18] suggest that  $\nu$ -dependent correlations in the electronic ground state may be responsible for the observed effects.

The analyzed device consists of a charge-tunable MoSe<sub>2</sub> monolayer that is encapsulated between two hexagonal boron nitride (hBN) layers and two few-layer-graphene (FLG) gates; the structure is deposited on sapphire substrate [see Fig. 1(a) and Ref. [18] for details]. For the experiments, the device was mounted in a dilution refrigerator with a monomode-fiber-based optical access [18] allowing us to perform polarization-resolved, magneto-optical experiments at a base temperature  $T_b$  of either 80 mK or 4 K (note that the actual electronic temperature  $T$  in the former case is larger, possibly reaching a few hundreds of millikelvins [29,30]) [31]. In case of the reflectance measurements, the sample was illuminated with a light emitting diode featuring a center wavelength of 760 nm and 20-nm linewidth. The resonant fluorescence (RF) and photoluminescence excitation (PLE) experiments were in turn performed with the use of a single-frequency, continuous-wave (CW) Ti-sapphire laser that was spectrally broadened using an electro-optic phase modulator

with a  $\sim 20$  GHz drive (to reduce the coherence length and the related etaloning, while retaining narrow linewidth  $< 0.1$  meV). All results presented in the main text were obtained at  $B = 14$  T for the spots in the central area of the device, i.e., away from its edges [see Supplemental Material (SM) [32] for complementary datasets acquired on different devices].

Figure 1(c) shows a representative top-gate-voltage ( $V_t$ ) evolution of the circular-polarization-resolved reflectance contrast  $\Delta R/R_0$  spectra taken at  $T_b = 80$  mK. In the charge-neutral regime (at  $-14\text{V} \lesssim V_t \lesssim 0$  V), the spectra display a single, bare exciton resonance ( $X$ ) that is split between the two circular polarizations by  $g_X^* \mu_B B$  due to the valley-Zeeman effect with  $g_X^* \approx 4.3$  [41,47,48]. Similarly, the valley degeneracy of both conduction and valence bands is lifted for  $B \neq 0$ . In a single-particle approximation [see Fig. 1(b)], the resulting splitting  $g_{e,h}^* \mu_B B$  of the lowest electron (hole) LLs is  $\approx 4$  meV ( $\approx 7$  meV) at  $B = 14$  T, assuming an effective  $g$  factor of  $g_e^* \approx 5$  ( $g_h^* \approx 9$ ) [2,41–43]. Therefore, the spin-valley splitting exceeds the thermal energy  $k_B T$  by more than an order of magnitude even at  $T_b = 4$  K. Consequently, at low doping densities the itinerant electrons (holes) are expected to be fully spin polarized and fill the states in  $K^-$  ( $K^+$ ) valley for  $B > 0$ . Under such conditions only the excitons in the opposite  $K^+$

( $K^-$ ) valley can get dressed into attractive (AP) and repulsive (RP) Fermi polarons [49,50], leading to the emergence of a redshifted AP resonance exclusively in  $\sigma^+$  ( $\sigma^-$ ) polarization.

While the above picture remains in perfect agreement with the optical response measured on the hole side (at  $V_i \lesssim -14$  V), in case of the electron doping (at  $V_i \gtrsim 0$  V) we clearly observe the AP resonances in both polarizations. Although the  $\sigma^+$ -polarized resonance ( $AP_+$ ) is much stronger than its  $\sigma^-$ -polarized counterpart ( $AP_-$ ), the latter exhibits pronounced intensity oscillations as the electron density  $n_e$  is varied, indicating that spin-valley polarization depends on the LL filling factor  $\nu$ . To quantitatively analyze this effect, we fit the line shapes of both resonances with a transfer-matrix approach (see SM [32]), which allows us to extract their oscillator strengths  $f_{AP\pm}$  being directly proportional to the densities  $n_e^\mp$  of electrons residing in  $K^\mp$  valleys [49,51,52]. Figures 1(e) and 1(f) display gate-voltage dependencies of the determined  $f_{AP\pm}$  along with the corresponding polarization degree  $\mathcal{P}_{AP} = (f_{AP_+} - f_{AP_-}) / (f_{AP_+} + f_{AP_-})$ . The AP intensity oscillations are directly correlated with  $\nu$ , as revealed by their coincidence with Shubnikov–de Haas oscillations of the  $K^-$  exciton linewidth [Fig. 1(d)] [53]. Specifically, the  $AP_-$  resonance is stronger around half-integer  $\nu$ , and becomes barely discernible for integer  $\nu$  (until  $\nu = 6$ , beyond which the Fermi energy exceeds the Zeeman splitting of the conduction band). These changes coincide with the periodic variations of the slope of the  $AP_+$  intensity increase, demonstrating that the electrons become partially spin-valley depolarized each time the highest-energy LL is partially occupied. Such depolarization turns out to be particularly prominent at  $\nu < 1$ , where  $\mathcal{P}_{AP}$  steeply decreases for lower  $n_e$ , reaching almost zero in the zero-density limit. Interestingly, this initial drop of  $\mathcal{P}_{AP}$  becomes suppressed upon rising the temperature to  $T_b = 4$  K. This observation is in stark contrast to naive expectation that electronic spin depolarization would be enhanced by thermal fluctuations. At elevated  $T$  the density-dependent polarization variation also becomes clearly less pronounced [see Fig. 1(f)].

This unusual temperature dependence suggests that the observed valley depolarization does not occur in the ground state of the electron system. To verify this claim, we repeat reflectance measurements at  $T_b = 80$  mK for different powers of the white-light excitation. As shown in Figs. 2(a) and 2(b), the amplitude of  $\nu$ -dependent oscillations of  $\mathcal{P}_{AP}$  and  $f_{AP_-}$  markedly increases for larger powers. Concurrently, the oscillations become indiscernible for powers lower than a few nanowatts, but the initial drop of  $\mathcal{P}_{AP}$  at low  $\nu < 1$  remains pronounced even below 1 nW. Given that all utilized excitation powers are significantly lower than those required to sizably heat the electron system [30], these observations indicate that the loss of electron spin-valley polarization arises due to exciton-mediated spin-valley-flip of electrons.

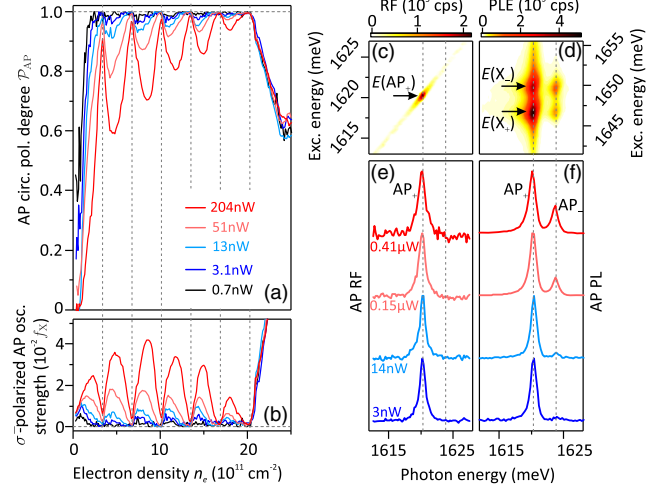


FIG. 2. (a),(b)  $\mathcal{P}_{AP}$  (a) and  $f_{AP_-}$  (b) determined as a function of  $n_e$  based on  $\Delta R/R_0$  measurements carried out at  $T_b = 80$  mK,  $B = 14$  T, and for different powers of the white-light excitation [the exploited white-light spectrum is shown in Fig. 1(c)]. Vertical dashed lines mark subsequent integer filling factors. (c),(d) Color-scale plots displaying the AP RF (c) and PL (d) excited using linearly polarized, spectrally narrow laser with power of  $0.15 \mu\text{W}$ . The spectra were detected in orthogonal linear polarization, for fixed  $\nu \approx 0.8$ , and at the same  $B$  and  $T_b$  as in panels (a),(b). In both plots the dark counts of the CCD camera were subtracted. The RF data were additionally corrected for background signal stemming from imperfectly suppressed laser by subtracting the reference RF signal measured at charge neutrality. (e),(f) The AP RF (e) and PL spectra (f; quasiresonantly excited via the higher-energy  $X_-$  resonance and averaged over 2-meV-wide excitation energy window) obtained for different powers of the tunable laser. For clarity, the spectra are vertically offset and normalized.

In order to support this conclusion and further exclude any heating-related origin of the investigated effect, we perform RF measurements of the AP resonance using a spectrally narrow tunable laser. In these experiments the gate voltage is fixed at a value corresponding to  $\nu \approx 0.8$ . Moreover, the reflected light is collected in cross-linear-polarization with respect to the laser, which enables us to suppress the laser background and to address  $AP_+$  and  $AP_-$  transitions with equal probabilities. In such a resonant scheme, each of the  $AP_\pm$  resonances may be excited only if there are electrons residing in the  $K^\mp$  valley in the absence of the excitons. Figure 2(c) displays an example RF spectrum acquired under such conditions. It features only one, lower-energy  $AP_+$  resonance, which demonstrates complete polarization of the electrons in their ground state. This finding remains valid independently of the utilized laser power [Fig. 2(e)], including the powers for which the electrons are already sizably depolarized under broadband white-light excitation [cf. Fig. 2(a)]. Furthermore, the electronic depolarization is also induced by the resonant laser when its energy is tuned to either of the two Zeeman-split

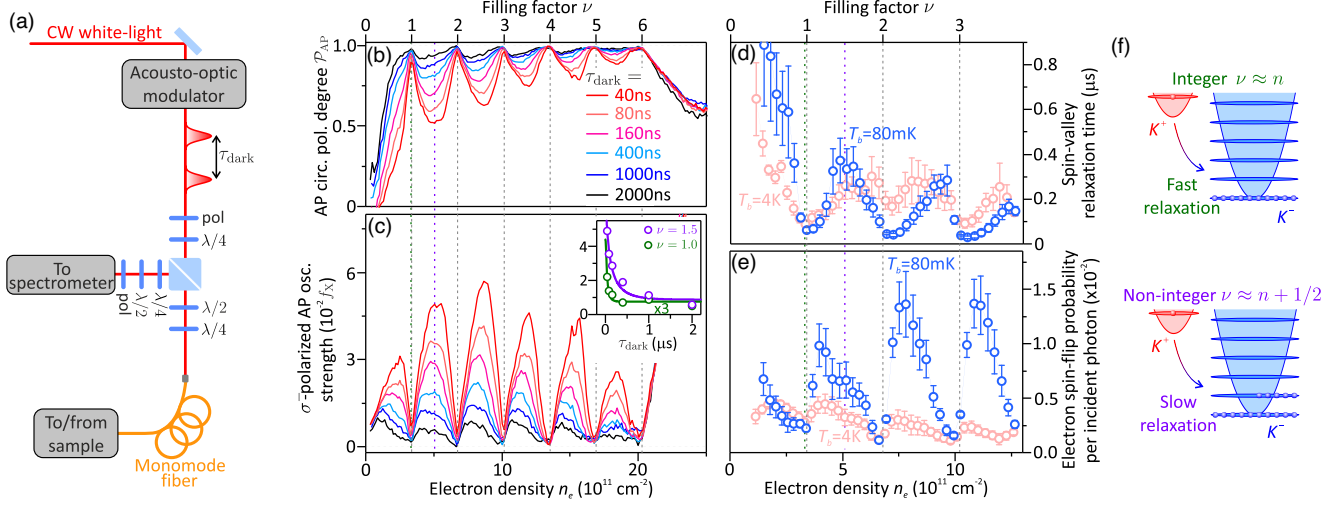


FIG. 3. (a) Simplified illustration of the experimental setup used in time-resolved measurements of electron relaxation dynamics. (b),(c) Electron-density dependence of  $\mathcal{P}_{\text{AP}}$  (b) and  $f_{\text{AP}_-}$  (c) obtained for different  $\tau_{\text{dark}}$  at  $B = 14$  T and  $T_b = 80$  mK. The inset in panel (c) displays  $f_{\text{AP}_-}$  determined for two selected  $\nu = 1.0$  and  $1.5$  versus  $\tau_{\text{dark}}$  (note that the former dataset was multiplied by 3). The solid lines represent the fits of the data with the rate equation model (see SM [32]). (d),(e) The values of the relaxation time  $\tau_{\text{relax}}$  (d) and spin-flip probability  $p_{\text{flip}}$  (e) determined as a function of  $n_e$  at  $B = 14$  T for two different temperatures  $T_b = 80$  mK and  $T_b = 4$  K (the data were binned in  $\Delta\nu \approx 0.1$  increments). (f) Cartoons schematically illustrating the filling factors at which  $\tau_{\text{relax}}$  is shorter and longer.

exciton states ( $X_{\pm}$ ). This is revealed by Figs. 2(d) and 2(f) presenting the corresponding AP PL spectra obtained under such excitation conditions, where we observe both  $\text{AP}_{\pm}$  peaks with their intensity ratio increasing with the laser power.

The above results unequivocally demonstrate that—otherwise fully spin polarized— itinerant electrons undergo spin-valley flips in the presence of optically injected excitons. After each spin-flip event, an electron remains in the  $K^+$  valley until it relaxes back to the  $K^-$  one, which gives rise to a finite electron spin depolarization probed in our time-integrated studies. The corresponding depolarization degree is naturally expected to increase for low  $n_e$  (when the electrons with flipped spins constitute a larger fraction of the total  $n_e$ ), partially explaining why  $\mathcal{P}_{\text{AP}}$  exhibits a sharp decrease around low  $\nu$ . At the same time, the depolarization efficiency is also proportional to both the exciton injection rate (i.e., excitation power) and the spin-valley relaxation time  $\tau_{\text{relax}}$ . Since the latter has been previously demonstrated to be longer for the holes (presumably owing to their larger spin-orbit splitting) [26,27], one may expect the depolarization in this case to be more efficient than for the electrons. This conjecture remains in stark contrast with our experimental results [cf. Fig. 1(c)], indicating that it is a difference in the exciton-induced carrier spin-flip rates that is a dominant factor responsible for more prominent electron spin depolarization. We speculate that the larger light-induced electron spin-flip probability  $p_{\text{flip}}$  (per one incident photon) stems from a very small splitting between the bright and dark intravalley excitons with the opposite electron spin orientation [55,56]: if these states had the same energy, spin-orbit interaction

could turn a bright exciton into an intravalley dark one, and upon spin-preserving valley relaxation of the electron, an intervalley dark exciton may be formed. Upon subsequent recombination of the hole with a same-valley Fermi-see electron, a net valley-flip excitation would be generated.

Taking advantage of the opportunity to drive the electrons out of equilibrium, we analyze their spin-valley dynamics. To this end we perform a time-resolved experiment [Fig. 3(a)], in which we monitor the steady-state reflectance contrast spectra excited with a train of equidistant,  $\sim 16$ -ns-long Gaussian white-light pulses separated by a dark period  $\tau_{\text{dark}}$ , which are produced by an acousto-optic modulator. Figures 3(b) and 3(c) present the  $n_e$  evolution of  $\mathcal{P}_{\text{AP}}$  and  $f_{\text{AP}_-}$  obtained at  $T_b = 80$  mK for a fixed pulse intensity but different  $\tau_{\text{dark}}$ . As expected, the  $\nu$ -dependent oscillations of both quantities become less prominent for longer  $\tau_{\text{dark}}$ . Moreover, the decrease of  $f_{\text{AP}_-}$  with  $\tau_{\text{dark}}$  turns out to be markedly different for various  $\nu$  [see inset to Fig. 3(c)]. In general, this might be a consequence of the  $n_e$  variation of either  $\tau_{\text{relax}}$  or  $p_{\text{flip}}$ , as both of these quantities influence the dependence of  $f_{\text{AP}_-}$  on  $\tau_{\text{dark}}$ . In order to disentangle these two contributions, we fit the  $f_{\text{AP}_-}(\tau_{\text{dark}})$  obtained at each  $n_e$  using a simple rate equation model with  $\tau_{\text{relax}}(n_e)$  and  $p_{\text{flip}}(n_e)$  being the only parameters (except for a global,  $n_e$ -independent scaling factor; see SM [32]). The fitting is carried out at low  $\nu < 4$  range, where the light-induced depolarization is particularly efficient.

As shown in Figs. 3(d) and 3(e), both of the extracted parameters exhibit prominent oscillations with  $\nu$ . The relaxation time is the shortest when the highest-energy

$n$ th LL is completely filled and becomes markedly prolonged around noninteger  $\nu$ . Depolarization probability undergoes similar oscillations. However, its evolution between subsequent integer  $\nu$  displays a more asymmetric shape:  $p_{\text{flip}}$  steeply increases from its minimum as soon as  $(n + 1)$ th LL starts to be occupied and then slowly decreases reaching another minimum at  $\nu = n + 1$ . These periodic fluctuations of both quantities lead to larger (smaller) steady-state spin polarization around integer (noninteger)  $\nu$ , which gives rise to the oscillating electron depolarization degree. A clearly different profile of  $\nu$ -dependent variation of  $\tau_{\text{relax}}$  and  $p_{\text{flip}}$  is also partially responsible for the prominent shift of the minimum of  $\mathcal{P}_{\text{AP}}(\nu)$  toward integer  $\nu$  when prolonging  $\tau_{\text{dark}}$  [cf. Fig. 3(b)].

The oscillations of  $\tau_{\text{relax}}$  and  $p_{\text{flip}}$  are found to be suppressed upon raising the temperature to  $T_b = 4$  K for  $\nu \gtrsim 1$  [Figs. 3(d) and 3(e)]. This effect is a few times more pronounced in case of  $p_{\text{flip}}$ , which displays a clear decreasing tendency at 4 K. The relaxation time, in turn, still exhibits a weak oscillatory behavior in this regime, yielding around 100–300 ns for the analyzed  $1 \lesssim \nu \lesssim 4$  range. These values remain in agreement with  $\tau_{\text{relax}}$  determined for various TMD monolayers in some of the previous reports [25–27].

In the following, we discuss possible mechanisms behind the variation of  $\tau_{\text{relax}}$ , which, unlike  $p_{\text{flip}}$ , constitutes an inherent property of the excited electron system. Owing to spin-valley locking, phonon-mediated relaxation of the excited states in TMD monolayers is strongly suppressed at low temperatures by energy-momentum conservation. Even though we cannot experimentally rule out the influence of coupling to a phonon reservoir on the spin relaxation dynamics, its marked ground-state dependence hints at a central role played by electronic correlations induced by strong Coulomb interactions. Such correlations are suppressed when the electrons form an IQH state at  $\nu = n$ , but may become pronounced whenever the system gets occupied by excess electrons or holes ( $\nu = n \pm \epsilon$ ) [57–59]. We speculate that this gives rise to substantially longer  $\tau_{\text{relax}}$  revealed by our millikelvin-temperature experiments at  $\nu \neq n$ . This speculation is consistent with a similar slowdown of the relaxation dynamics demonstrated previously for  $\text{WSe}_2/\text{WS}_2$  heterobilayer hosting a Mott-like CI state [10]. Our conjecture is further supported by recent experiments [18] showing evidence of the formation of the WC ground state in a monolayer system at  $B = 14$  T for  $\nu \lesssim 0.5$ , which is the  $\nu$  range where the prolongation of  $\tau_{\text{relax}}$  is the most prominent. The reported WC melting temperature exceeds 4 K, which may explain why the increase of  $\tau_{\text{relax}}$  in this regime is prominent both at millikelvin and 4 K temperatures. Reduced amplitude of  $\tau_{\text{relax}}$  oscillations at  $\nu > 1$  for  $T_b = 4$  K may in turn be a consequence of a more fragile nature of the corresponding correlated states.

The strong filling-factor dependence of spin-valley relaxation uncovered by our work paves the way toward

future explorations of nonequilibrium dynamics of electrons in atomically thin semiconductors. In parallel, the large efficiency of the  $\nu$ -dependent light-induced electron spin depolarization mechanism utilized in our experiments indicates that excitons might not constitute a nondestructive probe of the electronic system in TMD monolayers even when the electron density is orders of magnitude larger than that of the excitons.

The data that support the findings of this Letter are available in the ETH Research Collection [60].

We thank P. Back, A. Popert, and X. Lu for fabricating the investigated devices. This work was supported by the Swiss National Science Foundation (SNSF) under Grant No. 200021\_204076 and as a part of NCCR QSIT, a National Centre of Competence (or Excellence) in Research, funded by the SNSF (Grant No. 51NF40-185902). K. W. and T. T. acknowledge support from the Elemental Strategy Initiative conducted by the MEXT, Japan (Grant No. JPMXP0112101001) and JSPS KAKENHI (Grants No. 19H05790 and No. JP20H00354).

\*Corresponding author.

tomaszs@phys.ethz.ch

- [1] K. F. Mak, C. Lee, J. Hone, J. Shan, and T. F. Heinz, *Phys. Rev. Lett.* **105**, 136805 (2010).
- [2] X. Xu, W. Yao, D. Xiao, and T. F. Heinz, *Nat. Phys.* **10**, 343 (2014).
- [3] T. C. Berkelbach, M. S. Hybertsen, and D. R. Reichman, *Phys. Rev. B* **88**, 045318 (2013).
- [4] A. Chernikov, T. C. Berkelbach, H. M. Hill, A. Rigosi, Y. Li, O. B. Aslan, D. R. Reichman, M. S. Hybertsen, and T. F. Heinz, *Phys. Rev. Lett.* **113**, 076802 (2014).
- [5] D. Xiao, G.-B. Liu, W. Feng, X. Xu, and W. Yao, *Phys. Rev. Lett.* **108**, 196802 (2012).
- [6] T. Cao, G. Wang, W. Han, H. Ye, C. Zhu, J. Shi, Q. Niu, P. Tan, E. Wang, B. Liu, and J. Feng, *Nat. Commun.* **3**, 887 (2012).
- [7] H. Zeng, J. Dai, W. Yao, D. Xiao, and X. Cui, *Nat. Nanotechnol.* **7**, 490 (2012).
- [8] K. Mak, K. He, J. Shan, and T. F. Heinz, *Nat. Nanotechnol.* **7**, 494 (2012).
- [9] Y. Tang, L. Li, T. Li, Y. Xu, S. Liu, K. Barmak, K. Watanabe, T. Taniguchi, A. H. MacDonald, J. Shan, and K. F. Mak, *Nature (London)* **579**, 353 (2020).
- [10] E. C. Regan, D. Wang, C. Jin, M. I. Bakti Utama, B. Gao, X. Wei, S. Zhao, W. Zhao, Z. Zhang, K. Yumigeta, M. Blei, J. D. Carlström, K. Watanabe, T. Taniguchi, S. Tongay, M. Crommie, A. Zettl, and F. Wang, *Nature (London)* **579**, 359 (2020).
- [11] Y. Shimazaki, I. Schwartz, K. Watanabe, T. Taniguchi, M. Kroner, and A. Imamoğlu, *Nature (London)* **580**, 472 (2020).
- [12] L. Wang, E.-M. Shih, A. Ghiotto, L. Xian, D. A. Rhodes, C. Tan, M. Claassen, D. M. Kennes, Y. Bai, B. Kim, K. Watanabe, T. Taniguchi, X. Zhu, J. Hone, A. Rubio, A. N. Pasupathy, and C. R. Dean, *Nat. Mater.* **19**, 861 (2020).

- [13] Y. Shimazaki, C. Kuhlenkamp, I. Schwartz, T. Smoleński, K. Watanabe, T. Taniguchi, M. Kroner, R. Schmidt, M. Knap, and A. Imamoğlu, *Phys. Rev. X* **11**, 021027 (2021).
- [14] Y. Cao, V. Fatemi, S. Fang, K. Watanabe, T. Taniguchi, E. Kaxiras, and P. Jarillo-Herrero, *Nature (London)* **556**, 43 (2018).
- [15] Y. Cao, V. Fatemi, A. Demir, S. Fang, S. L. Tomarken, J. Y. Luo, J. D. Sanchez-Yamagishi, K. Watanabe, T. Taniguchi, E. Kaxiras, R. C. Ashoori, and P. Jarillo-Herrero, *Nature (London)* **556**, 80 (2018).
- [16] X. Lu, P. Stepanov, W. Yang, M. Xie, M. A. Aamir, I. Das, C. Urgell, K. Watanabe, T. Taniguchi, G. Zhang, A. Bachtold, A. H. MacDonald, and D. K. Efetov, *Nature (London)* **574**, 653 (2019).
- [17] Y. Xu, S. Liu, D. A. Rhodes, K. Watanabe, T. Taniguchi, J. Hone, V. Elser, K. F. Mak, and J. Shan, *Nature (London)* **587**, 214 (2020).
- [18] T. Smoleński, P. E. Dolgirev, C. Kuhlenkamp, A. Popert, Y. Shimazaki, P. Back, X. Lu, M. Kroner, K. Watanabe, T. Taniguchi, I. Esterlis, E. Demler, and A. Imamoğlu, *Nature (London)* **595**, 53 (2021).
- [19] Y. Zhou, J. Sung, E. Brutschea, I. Esterlis, Y. Wang, G. Scuri, R. J. Gelly, H. Heo, T. Taniguchi, K. Watanabe, G. Zaránd, M. D. Lukin, P. Kim, E. Demler, and H. Park, *Nature (London)* **595**, 48 (2021).
- [20] Q. Shi, E.-M. Shih, M. V. Gustafsson, D. A. Rhodes, B. Kim, K. Watanabe, T. Taniguchi, Z. Papić, J. Hone, and C. R. Dean, *Nat. Nanotechnol.* **15**, 569 (2020).
- [21] L. Yang, N. A. Sinitsyn, W. Chen, J. Yuan, J. Zhang, J. Lou, and S. A. Crooker, *Nat. Phys.* **11**, 830 (2015).
- [22] W.-T. Hsu, Y.-L. Chen, C.-H. Chen, P.-S. Liu, T.-H. Hou, L.-J. Li, and W.-H. Chang, *Nat. Commun.* **6**, 8963 (2015).
- [23] T. Yan, S. Yang, D. Li, and X. Cui, *Phys. Rev. B* **95**, 241406 (R) (2017).
- [24] E. J. McCormick, M. J. Newburger, Y. K. Luo, K. M. McCreary, S. Singh, I. B. Martin, E. J. Cichewicz Jr., B. T. Jonker, and R. K. Kawakami, *2D Mater.* **5**, 011010 (2017).
- [25] X. Song, S. Xie, K. Kang, J. Park, and V. Sih, *Nano Lett.* **16**, 5010 (2016).
- [26] P. Dey, L. Yang, C. Robert, G. Wang, B. Urbaszek, X. Marie, and S. A. Crooker, *Phys. Rev. Lett.* **119**, 137401 (2017).
- [27] M. Goryca, N. P. Wilson, P. Dey, X. Xu, and S. A. Crooker, *Sci. Adv.* **5**, eaau4899 (2019).
- [28] J. Li, M. Goryca, K. Yumigeta, H. Li, S. Tongay, and S. A. Crooker, *Phys. Rev. Mater.* **5**, 044001 (2021).
- [29] C. Latta, F. Haupt, M. Hanl, A. Weichselbaum, M. Claassen, W. Wuester, P. Fallahi, S. Faelt, L. Glazman, J. von Delft, H. E. Türeci, and A. Imamoğlu, *Nature (London)* **474**, 627 (2011).
- [30] F. Haupt, A. Imamoğlu, and M. Kroner, *Phys. Rev. Applied* **2**, 024001 (2014).
- [31] While the electronic temperature  $T$  was not directly extracted in the reported experiments, extrapolating from our earlier measurements performed in the same setup, we estimate that  $200 \text{ mK} \lesssim T < 1 \text{ K}$  for  $T_b = 80 \text{ mK}$ .
- [32] See Supplemental Material at <http://link.aps.org/supplemental/10.1103/PhysRevLett.128.127402> for further information concerning data analysis, calibration of the electron doping density, rate-equation modelling of time-resolved data as well as complementary datasets obtained on different devices, which includes Refs. [33–40].
- [33] P. Back, S. Zeytinoglu, A. Ijaz, M. Kroner, and A. Imamoğlu, *Phys. Rev. Lett.* **120**, 037401 (2018).
- [34] G. Scuri, Y. Zhou, A. A. High, D. S. Wild, C. Shu, K. De Greve, L. A. Jauregui, T. Taniguchi, K. Watanabe, P. Kim, M. D. Lukin, and H. Park, *Phys. Rev. Lett.* **120**, 037402 (2018).
- [35] S.-Y. Lee, T.-Y. Jeong, S. Jung, and K.-J. Yee, *Phys. Status Solidi (b)* **256**, 1800417 (2019).
- [36] T. Jakubczyk, V. Delmonte, M. Koperski, K. Nogajewski, C. Faugeras, W. Langbein, M. Potemski, and J. Kasprzak, *Nano Lett.* **16**, 5333 (2016).
- [37] H. H. Fang, B. Han, C. Robert, M. A. Semina, D. Lagarde, E. Courtade, T. Taniguchi, K. Watanabe, T. Amand, B. Urbaszek, M. M. Glazov, and X. Marie, *Phys. Rev. Lett.* **123**, 067401 (2019).
- [38] K. K. Kim, A. Hsu, X. Jia, S. M. Kim, Y. Shi, M. Dresselhaus, T. Palacios, and J. Kong, *ACS Nano* **6**, 8583 (2012).
- [39] A. Laturia, M. L. Van de Put, and W. G. Vandenberghe, *npj 2D Mater. Appl.* **2**, 6 (2018).
- [40] J. Zhu, T. Li, A. F. Young, J. Shan, and K. F. Mak, *Phys. Rev. Lett.* **127**, 247702 (2021).
- [41] G. Aivazian, Z. Gong, A. M. Jones, R.-L. Chu, J. Yan, D. G. Mandrus, C. Zhang, D. Cobden, W. Yao, and X. Xu, *Nat. Phys.* **11**, 148 (2015).
- [42] D. MacNeill, C. Heikes, K. F. Mak, Z. Anderson, A. Kormányos, V. Zólyomi, J. Park, and D. C. Ralph, *Phys. Rev. Lett.* **114**, 037401 (2015).
- [43] M. Koperski, M. R. Molas, A. Arora, K. Nogajewski, M. Bartos, J. Wyzula, D. Vaclavkova, P. Kossacki, and M. Potemski, *2D Mater.* **6**, 015001 (2018).
- [44] S. Larentis, H. C. P. Movva, B. Fallahzad, K. Kim, A. Behroozi, T. Taniguchi, K. Watanabe, S. K. Banerjee, and E. Tutuc, *Phys. Rev. B* **97**, 201407(R) (2018).
- [45] Y. Zhang, T.-R. Chang, B. Zhou, Y.-T. Cui, H. Yan, Z. Liu, F. Schmitt, J. Lee, R. Moore, Y. Chen, H. Lin, H.-T. Jeng, S.-K. Mo, Z. Hussain, A. Bansil, and Z.-X. Shen, *Nat. Nanotechnol.* **9**, 111 (2014).
- [46] M. Goryca, J. Li, A. V. Stier, T. Taniguchi, K. Watanabe, E. Courtade, S. Shree, C. Robert, B. Urbaszek, X. Marie, and S. A. Crooker, *Nat. Commun.* **10**, 4172 (2019).
- [47] Y. Li, J. Ludwig, T. Low, A. Chernikov, X. Cui, G. Arefe, Y. D. Kim, A. M. van der Zande, A. Rigosi, H. M. Hill, S. H. Kim, J. Hone, Z. Li, D. Smirnov, and T. F. Heinz, *Phys. Rev. Lett.* **113**, 266804 (2014).
- [48] A. Srivastava, M. Sidler, A. V. Allain, D. S. Lembke, A. Kis, and A. Imamoğlu, *Nat. Phys.* **11**, 141 (2015).
- [49] M. Sidler, P. Back, O. Cotlet, A. Srivastava, T. Fink, M. Kroner, E. Demler, and A. Imamoğlu, *Nat. Phys.* **13**, 255 (2017).
- [50] D. K. Efimkin and A. H. MacDonald, *Phys. Rev. B* **95**, 035417 (2017).
- [51] M. M. Glazov, *J. Chem. Phys.* **153**, 034703 (2020).
- [52] A. Imamoğlu, O. Cotlet, and R. Schmidt, *C. R. Phys.* **22**, 1 (2021).
- [53] We use the minima of the  $K^-$  exciton linewidth, which occur precisely at integer  $\nu$  [54], to calibrate  $n_e$ , see SM [32] for details.

- [54] T. Smoleński, O. Cotlet, A. Popert, P. Back, Y. Shimazaki, P. Knüppel, N. Dietler, T. Taniguchi, K. Watanabe, M. Kroner, and A. Imamoglu, *Phys. Rev. Lett.* **123**, 097403 (2019).
- [55] Z. Lu, D. Rhodes, Z. Li, D. Van Tuan, Y. Jiang, J. Ludwig, Z. Jiang, Z. Lian, S.-F. Shi, J. Hone, H. Dery, and D. Smirnov, *2D Mater.* **7**, 015017 (2019).
- [56] C. Robert, B. Han, P. Kapuscinski, A. Delhomme, C. Faugeras, T. Amand, M. R. Molas, M. Bartos, K. Watanabe, T. Taniguchi, B. Urbaszek, M. Potemski, and X. Marie, *Nat. Commun.* **11**, 4037 (2020).
- [57] A. A. Koulakov, M. M. Fogler, and B. I. Shklovskii, *Phys. Rev. Lett.* **76**, 499 (1996).
- [58] M. M. Fogler, A. A. Koulakov, and B. I. Shklovskii, *Phys. Rev. B* **54**, 1853 (1996).
- [59] M. M. Fogler, in *High Magnetic Fields* (Springer, Berlin, Heidelberg, 2002), Vol. 595, pp. 98–138.
- [60] T. Smoleński, M. Kroner, and A. Imamoglu, ETH Research Collection, <http://hdl.handle.net/20.500.11850/530293> (2022).